RESEARCH ARTICLE | APRIL 07 2025

# Non-Newtonian Casson liquid induced by dust particles with hybrid nano fluid over a stretching sheet

Devaki Palluru; Kaarimah; Rahul Das

*AIP Conf. Proc.* 3283, 040002 (2025)
https://doi.org/10.1063/5.0265165





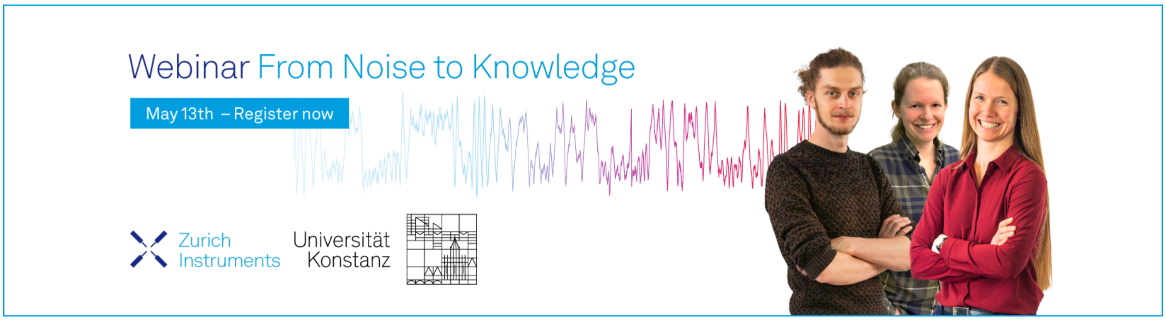

# Non-Newtonian Casson Liquid Induced by Dust Particles with Hybrid Nano Fluid over a Stretching Sheet

Devaki Palluru[1, a)] Kaarimah[1, b)] *and* Rahul Das[1c)]

[1] *Sri Venkateswara College, University of Delhi, New Delhi* – 110021, *INDIA*

[a)]Corresponding author: p.devaki@svc.ac.in
[b)]kaarimahnaqash46@gmail.com
[c)]rahuldas2262003@gmail.com

**Abstract.** This research paper investigates the behavior of a Non-Newtonian Casson fluid with dust particles on a stretched sheet, in the presence of hybrid nanofluid. The study aims to understand the impact of various physical parameters on fluid and dust particle velocity. Analytical solutions with appropriate boundary conditions are employed to solve the governing equations. The results reveal that higher fluid-particle interaction leads to increased dust particle velocity, attributed to yield stress and hybrid nanofluid effects. The research provides valuable insights into the complex dynamics of the flow, emphasizing the significance of factors like fluid-particle interaction, Casson parameter, and magnetic properties. Graphical analysis facilitates a clear understanding of these relationships. Overall, this study contributes to knowledge in stretching sheets and offers guidelines for researchers exploring non-Newtonian fluid behavior with dust particles.

**Keywords:** Casson Liquid, Hybrid Nano Fluid, Dust Particles, Stretching Sheet

## INTRODUCTION



The objective of this work is to study the fascinating behavior of the Casson fluid (CAF) and its interactions with different scenarios. The Casson fluid is a unique non-Newtonian fluid that exhibits interesting characteristics such as yield stress, shear-thinning behavior, and high viscosity. It can even mimic the behavior of a Newtonian fluid under certain conditions, making it an intriguing model for investigating viscosity manipulation and rheological behavior. In recent research, there has been a compelling correlation observed between the increase in the volume fraction of nanoparticles and the rise in dynamic viscosity. This finding suggests that the Casson fluid can be utilized as a valuable tool in characterizing the behavior of non-Newtonian fluids, finding applications in various domains. These domains include drag-reduction agents, printing technology, damping and braking devices, personal protective equipment, and even food products. The captivating tapestry of possibilities offered by non-Newtonian fluids showcases their versatility and potential in diverse fields.

Nanoparticles, on the other hand, possess their mesmerizing properties and find applications in fields such as medicine, agriculture, food production, and nuclear reactors. These nanoparticles, when dispersed harmoniously within conventional fluids, give rise to nanofluids. Nanofluids are formed by blending nano-sized particles with fluids like blood, water, engine oils, and ethylene glycol. However, selecting the ideal combination of nanoparticles is crucial for achieving stability within hybrid nanofluids. Metals like silver (Ag), copper (Cu), and metal oxides such as iron oxide (Fe203), copper oxide (CuO), and aluminum oxide (Al203) interweave with carbon materials like carbon nanotubes (CNTs), multi-walled carbon nanotubes (MWCNTs), and graphite to shape the landscape of both hybrid and regular nanofluid suspensions. Given the vast realm of fluid dynamics, researchers have delved into studying the captivating behavior of the Casson fluid and its interactions with various intriguing scenarios. This work aims to contribute to the understanding of the Casson fluid's behavior and its potential applications to pave the way for further advancements in fluid dynamics and nanofluid research.

The research paper is built upon the separate works of several authors. Mukhopadhyay [1] initially explored the impact of the Casson parameter on fluid velocity through an erratic stretching sheet. Building upon this, Bhattacharyya et al. [2] introduced the concept of double solutions in CAF flow with the addition of a permeable shrinking surface and radiation effects. Animasaun et al. [3] further investigated the influence of heat generation on CAF flow towards an exponentially stretched surface with mass suction, using the homotopy analysis method. The magnetic influence on the flow of Casson fluid through a moving orthogonal permeable disk was meticulously examined by Qureshi et al. [4]. Ahmad et al. [5] focused on the steady two-dimensional flow of CAF induced by a stretching plate while considering the presence of Newtonian heating. Additionally, Rostami et al. [6] explored the interplay of buoyancy effects near a stagnation-point flow on a vertical plate with water-based silica/alumina hybrid nanoparticles. Waini et al. [7] delved into the stability of hybrid nanofluids near a stagnation-point on an exponentially shrinking/stretching

*International Conference on Advances in Pure & Applied Mathematics (ICAPAM)*
AIP Conf. Proc. 3283, 040002-1–040002-8; https://doi.org/10.1063/5.0265165

sheet. Kumar et al. [8] studied the flow of a Maxwell nanofluid infused with MWCNT/SWCNT across a stretching sheet, taking magnetic dipole effects and thermal radiation into account. Gowda et al. [9] investigated the impact of thermophoretic particles deposited in a hybrid nanofluid suspended by ferrite nanomaterials encountered by an expanding or contracting moving rotating disc. Khan et al. [10] focused on unsteady Blasius Rayleigh Stokes flow in a hybrid nanofluid, considering a plate enveloped in a magnetic field and non-Fourier heat flux. Drawing from these separate works, the research paper explores the combination of the Casson fluid and a hybrid nanofluid infused with Fe304-MWCNT/H2O as they flow through a stretching sheet under the influence of the Lorentz force.

The paper aims to provide an exact solution, revealing the fluid and dust phase velocities of both the normal nanofluid (Fe304/H20) and the hybrid nanofluid (Fe304-MWCNT/H20), thereby enhancing our understanding of the fluidic landscape. The further relevant content of the research paper will delve deeper into this mesmerizing combination and its potential applications.

## MATHEMATICAL MODELLING

Fluid phase Continuity equation:

$$\textbf{Continuity Equation:} \quad \frac{\partial u(x,y)}{\partial x} + \frac{\partial v(x,y)}{\partial y} \tag{1}$$

Fluid phase Momentum equation:

**Momentum Equation:**

$$\begin{aligned} &\rho_{\text{hbnf}}\left(u(x,y)\frac{\partial u(x,y)}{\partial x} + v(x,y)\frac{\partial u(x,y)}{\partial y}\right) \\ &= \mu_{\text{hbnf}}\left(1+\frac{1}{\gamma_A}\right)\frac{\partial^2 u(x,y)}{\partial x^2} - \sigma_{\text{hbnf}} B_0^2 \mu \\ &\quad + K_A N_A\left(u_d(x,y) - u(x,y)\right) - \frac{\gamma}{K_p \mu} \end{aligned} \tag{2}$$

Dust phase continuity equation:

$$\textbf{Continuity Equation:} \quad \frac{\partial u_d(x,y)}{\partial x} + \frac{\partial v_d(x,y)}{\partial y} \tag{3}$$

Dust phase momentum equation:

**Momentum Equation:**

$$\begin{aligned} &m_A\left(u_d(x,y)\frac{\partial u_d(x,y)}{\partial x} + v_d(x,y)\frac{\partial u_d(x,y)}{\partial y}\right) \\ &= K_A\left(-u_d(x,y) + u(x,y)\right) \end{aligned} \tag{4}$$

Boundary conditions:

$$\text{Fluid phase:} \quad u(x,0) = u_w(x), \quad v(x,0) = 0 \tag{5}$$

$$u(x,y) \to 0, \quad u_d(x,y) \to 0, \quad v_d(x,y) \to v \quad \text{as } y \to \infty \tag{6}$$

Similarity variables and explanations:

$$u = bxF'(\xi), \quad v = -\sqrt{b\nu_f}F(\xi), \quad \xi = y\sqrt{\frac{b}{\nu_f}}$$

$$u_d = bxG'(\xi), \quad v_d = -\sqrt{\nu_f b}G(\xi)$$

where $\nu_f$ is the kinematic viscosity, $\xi$ is the pseudo-similarity variable,

$G$ and $F$ are the dimensionless functions for the dust and fluid phases, respectively.

Prime ($\prime$) signifies the derivative with respect to $\xi$.

Symbols:

$K_A$ - Stokes drag coefficient,
$N_A$ - dust particle number,
$m_A$ - mass of the dust particle,
$\gamma_A$ - non-Newtonian (Casson) parameter,
$\mu_{\text{hbnf}}$ - dynamic viscosity,
$\rho_{\text{hbnf}}$ - density,
$\sigma_{\text{hbnf}}$ - electrical conductivity.

Transforming equations (1)-(6) into following ODEs:

**Fluid phase:**

$$\frac{\mu_{\text{hbnf}}}{\mu_f}\frac{\rho_f}{\rho_{\text{hbnf}}}\left(1+\frac{1}{\gamma_A}\right)F'''+FF''-F'^2-\frac{\sigma_{\text{hbnf}}}{\sigma_f}\frac{\rho_f}{\rho_{\text{hbnf}}}M_AF'+L_A\beta\nu_A\frac{\rho_{\text{hbnf}}}{\rho_f}(G-F)-\frac{\gamma}{K_p}\frac{F'}{\rho_{\text{hbnf}}b}=0, \tag{7}$$

**Dust phase:**

$$G''G-G'^2-\beta\nu_A(G'-F')=0, \tag{8}$$

**with Boundary conditions:**

When $\xi=0$, the function $F(\xi)=0$ and the first derivative of the function $F'(\xi)=1$. As $\xi\to\infty$, the function $F'(\xi)\to 0$, the derivative of the function $G'(\xi)\to 0$, and the function $G(\xi)\to F(\xi)$.

The important parameters in the equation are $\beta\nu_A$, which represents the interaction between fluid particles in terms of velocity,$L_A$ , which represents the mass concentration of dust particles, and $M_A$, which represents the magnetic parameter. These parameters are defined mathematically as such.

$$\beta\nu_A=\frac{K_A}{bm_A},$$
$$L_A=\frac{N_Am_A}{\rho_f},$$
$$M_A=\frac{\sigma_fB_0^2}{\rho_fb}.$$

Here, $\beta\nu_A$ is the fluid particle interaction parameter for velocity, $L_A$ is the mass concentration of dust particles, and $M_A$ is the magnetic parameter.

## ANALYTICAL SOLUTION PROCEDURE

The main idea of this work is to outline the analytical solution procedure for a set of nonlinear coupled similarity ordinary differential equations (ODEs), along with the boundary conditions. These ODEs describe the behavior of dust and fluid phases. The general solution of these highlighted equations is expressed in a specific form, which will be further discussed and analyzed in the following sections. This solution procedure allows for a complete and exact solution of the system, providing insights into the behavior of the dust and fluid phases.

**Fluid phase:**

$$F(\xi)=A_1+A_2e^{-A_3\xi}, \tag{9}$$

**Dust phase:**

$$G(\xi)=A_4+A_5e^{-A_6\xi}, \tag{10}$$

The values of constants $A_j$ (j from 1 to 6) (which are positive) can be determined by substituting the given exponential solution into both the fluid and dust equations, considering the appropriate boundary conditions. After simplifying both equations for the fluid and dust phases, we get the following result.

$$A_1 = -A_2 = A_4 = \frac{1}{Z_A},$$
$$A_3 = A_6 = Z_A,$$
$$A_5 = -\frac{\beta \nu_A}{Z_A(1+\beta\nu_A)}.$$

In the above equations, the term $Z_A$ is explicitly demarcated as

$$Z_A = \pm\sqrt{\left(\frac{1}{\left(\frac{\mu_{\text{hbnf}}}{\mu_f}\left(1+\frac{1}{\gamma_A}\right)\right)}\right)\left(\frac{\rho_{\text{hbnf}}}{\rho_f} + \frac{\sigma_{\text{hbnf}}}{\sigma_f}\cdot M_A + \frac{LA\beta\nu_A}{1+\beta\nu_A} + \frac{\gamma\rho_f}{K_p b}\right)}.$$

The positive solution of $Z_A$ will be regarded as valid as it meets all the specified conditions, while the negative solution of $Z_A$ will be disregarded as it does not satisfy the criteria. Consequently, the applicable solution of $Z_A$ will be considered as follows:

$$Z_A = \sqrt{\left(\frac{1}{\left(\frac{\mu_{\text{hbnf}}}{\mu_f}\left(1+\frac{1}{\gamma_A}\right)\right)}\right)\left(\frac{\rho_{\text{hbnf}}}{\rho_f} + \frac{\sigma_{\text{hbnf}}}{\sigma_f}\cdot M_A + \frac{LA\beta\nu_A}{1+\beta\nu_A} + \frac{\gamma\rho_f}{K_p b}\right)}.$$

The fluid phase and dust phase can be solved analytically by replacing the different values of $A_j$ (for $j = 1,\ldots,6$) resulting in the final closed-form expression.

**Fluid phase:**

$$F[\xi] := \frac{1}{Z_A} - \frac{1}{Z_A}\cdot e^{-Z_A\xi} \tag{11}$$

**Dust phase:**

$$G[\xi] := \frac{1}{Z_A} - \left(\frac{\beta\nu_A}{Z_A(1+\beta\nu_A)}\right)\cdot e^{-Z_A\xi} \tag{12}$$

## RESULTS AND DISCUSSIONS

This section presents the analytical solution in graphical forms. The impact of the parameters $\beta\nu_A$, $M_A$, and $\gamma_A$ on fluid and dust velocity are observed graphically. The graphs are plotted using the software Mathematica. From the graph following observations are made:

- Fig (1) shows that an increase in fluid-particle interaction ($\beta\nu_A$) doesn't have much impact on fluid velocity but a drastic increase in dust velocity is noticed through Fig (2).

- As the Casson parameter ($\gamma_A$) increases, there is a decrease in the velocity of both fluid and dust, which is due to the yield stress property of Casson fluid. This can be noticed in Fig (3) and Fig (4).

- Fig (5) and Fig (6) are focused on the impact of magnetic properties on fluid velocity and dust velocity respectively. It is observed that in both figures, an increase in the magnetic parameter decreases velocity.

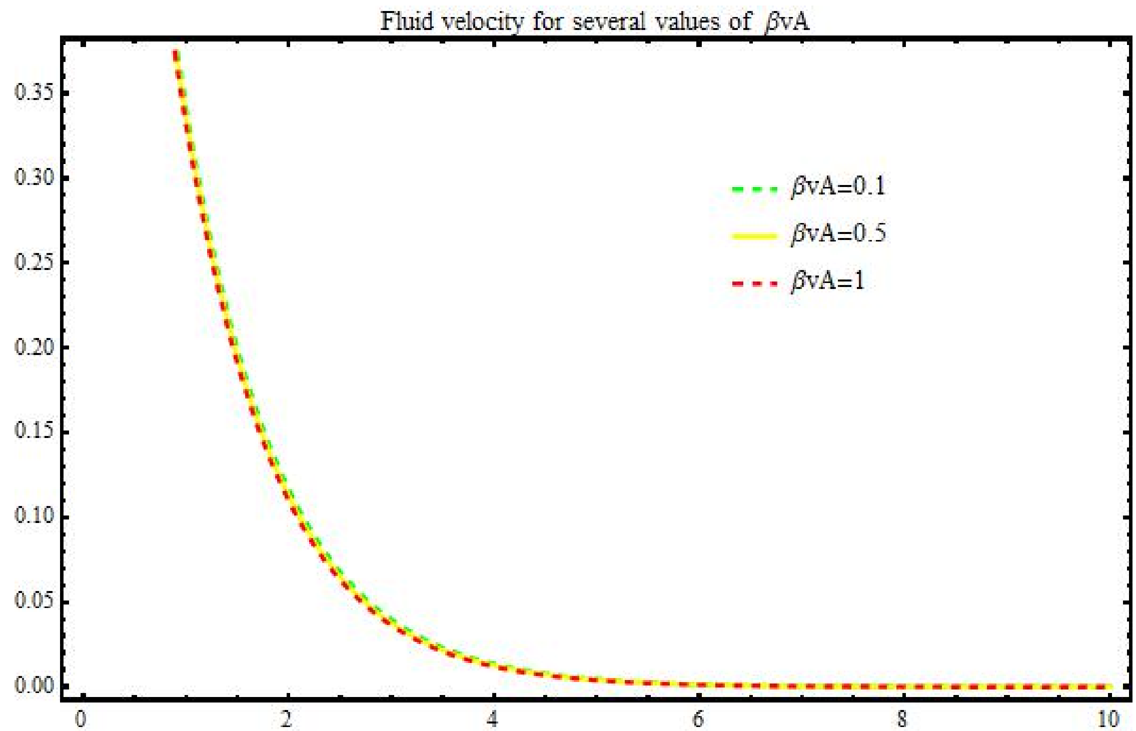


**FIGURE 1.** Fluid Velocity for several values of $\beta v_A$.

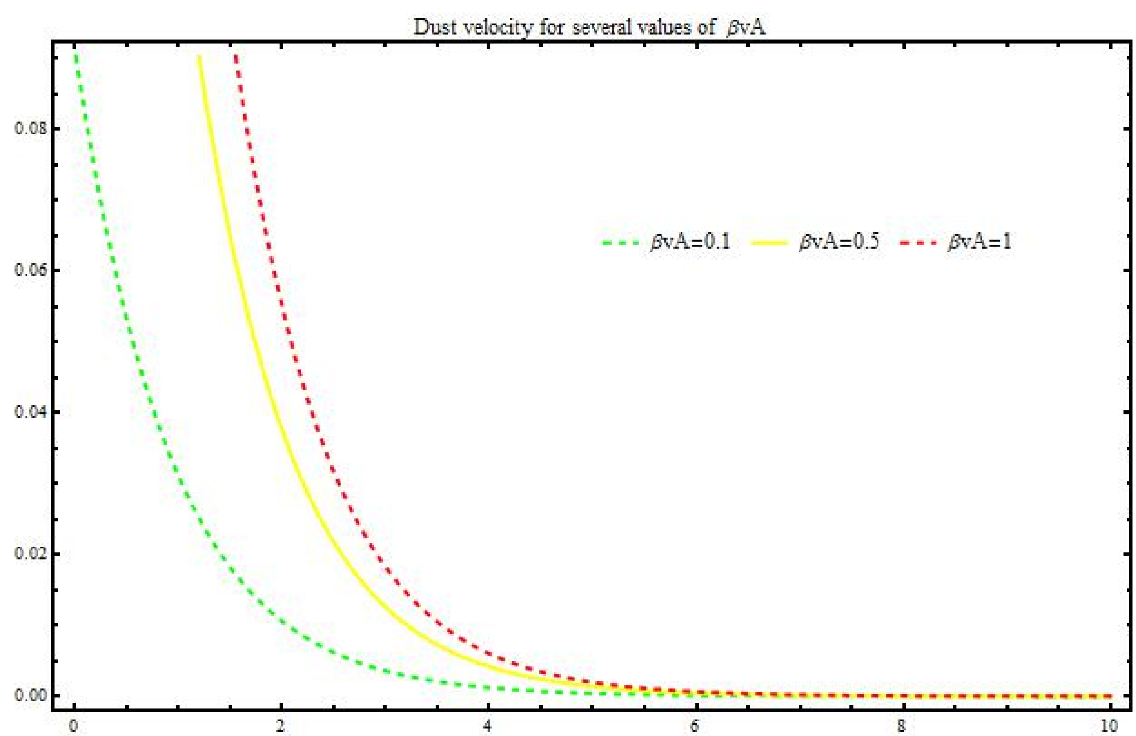


**FIGURE 2.** Dust Velocity for several values of $\beta v_A$.

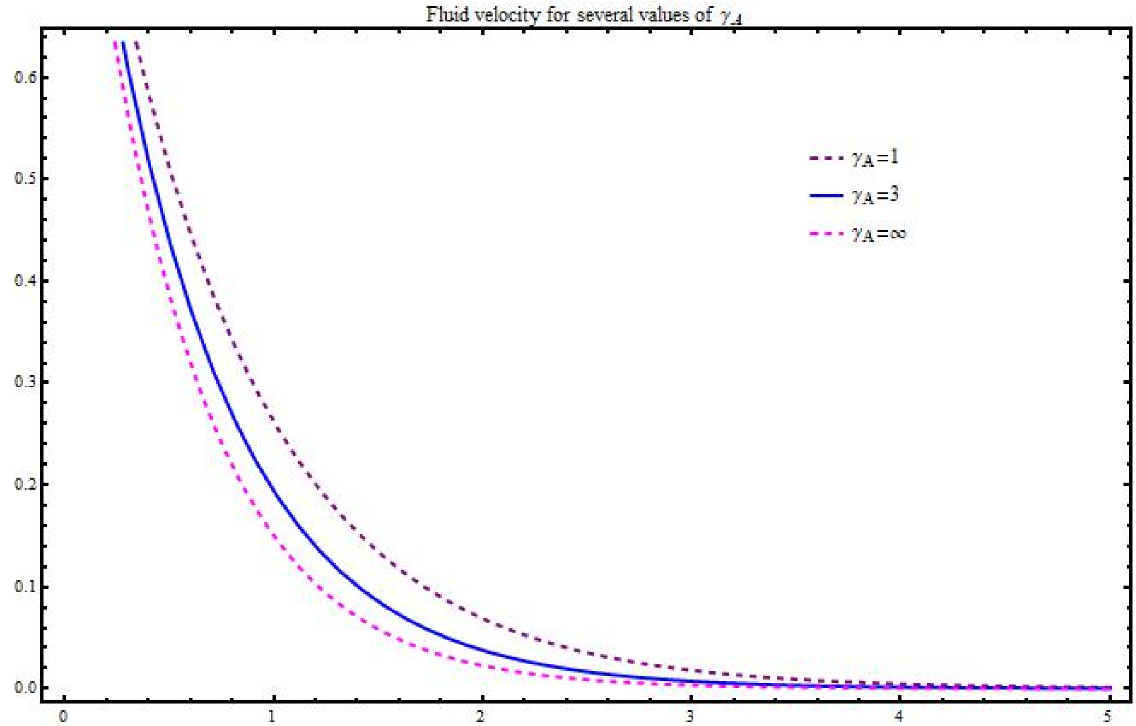


**FIGURE 3.** Fluid Velocity for several values of $\gamma_A$.

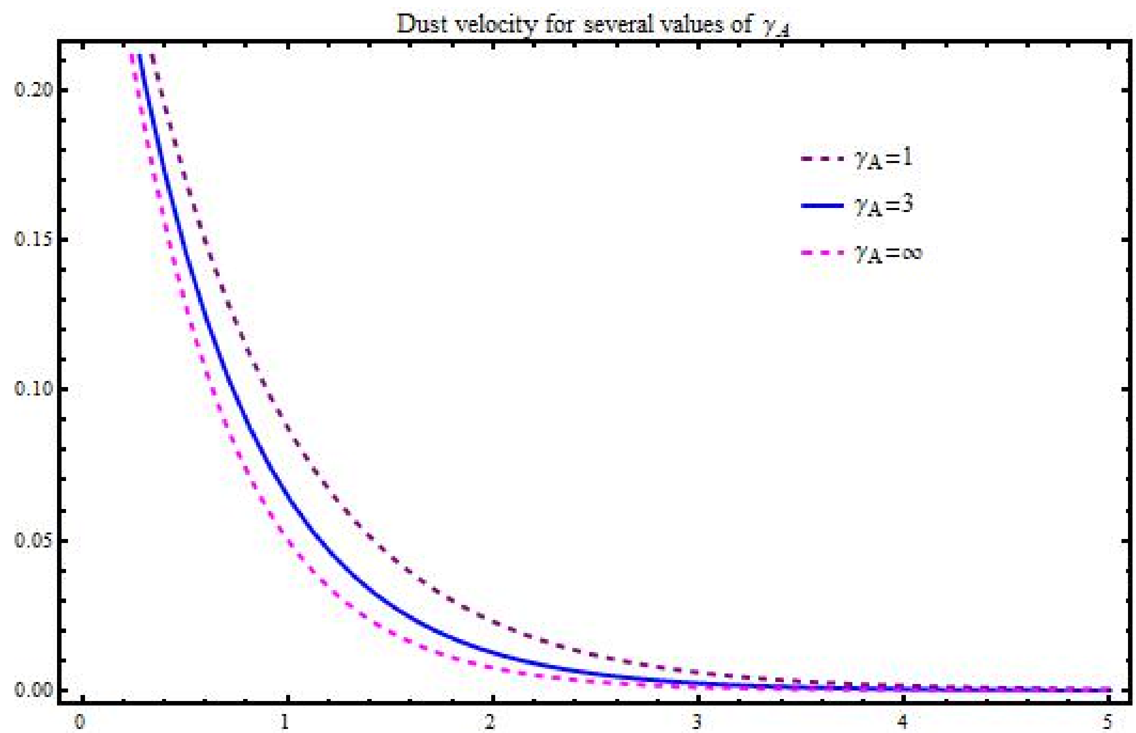


**FIGURE 4.** Dust Velocity for several values of $\gamma_A$.

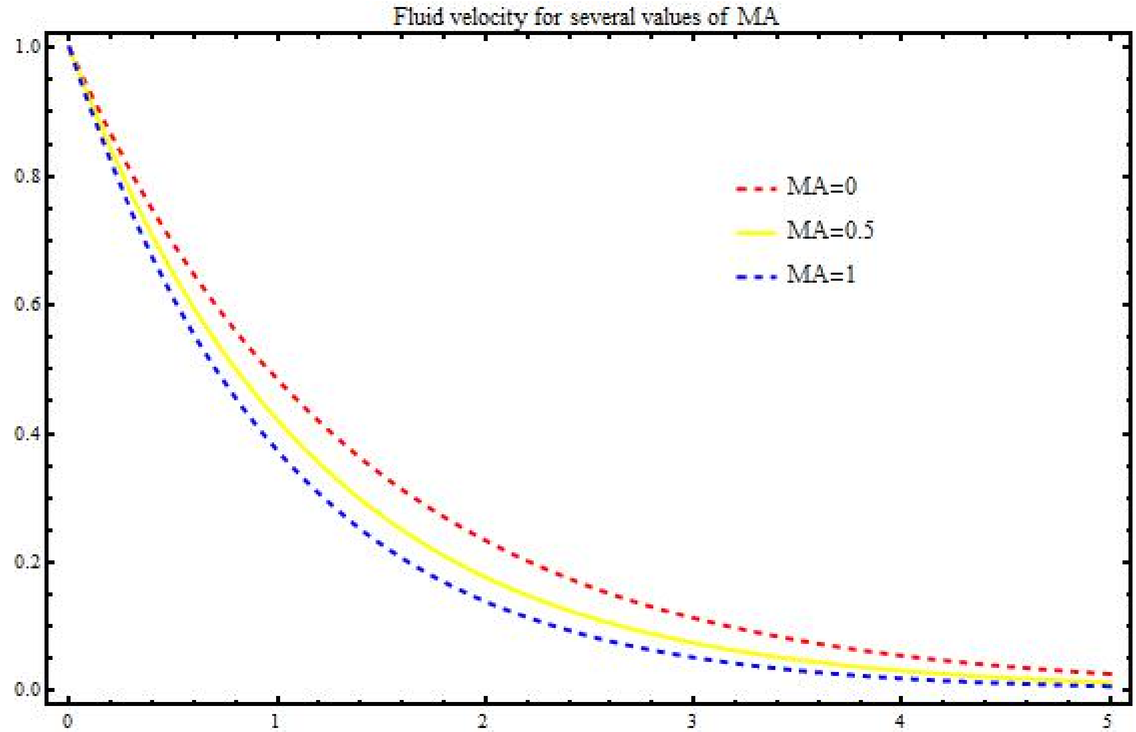


**FIGURE 5.** Fluid Velocity for several values of $M_A$.

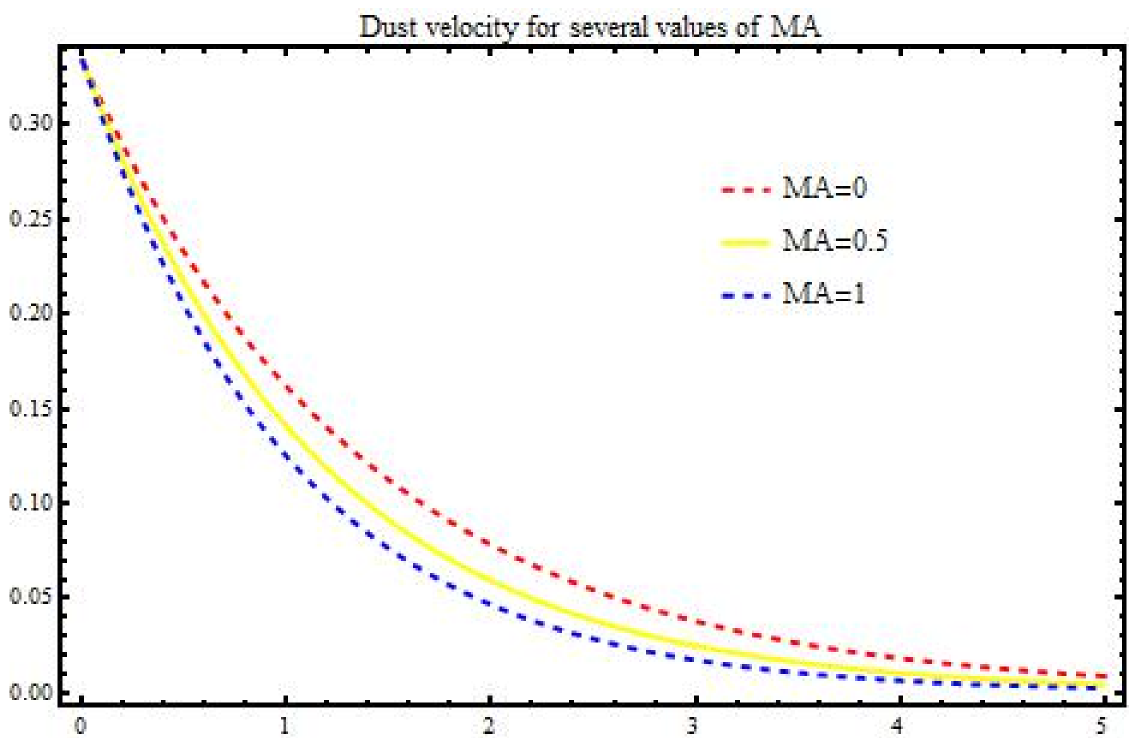


**FIGURE 6.** Dust Velocity for several values of $M_A$.

## CONCLUSIONS

Interesting observations are made graphically in the analytical approach of solving equations governing the flow of hybrid Casson Nanofluid inducted by dust particles over a sheet that is stretched. The velocity of dust particles and hybrid Casson Nanofluid is raised with a rise in yield stress and falls with a rise in magnetic parameters. One of the highlights of this work is dust velocity and particle interact parameters are traveling in the same direction.

## REFERENCES


1. M. S., "Casson fluid flow and heat transfer over a non-linearly stretching surface," 5(12) (2015).
2. B. K., U. MS, and L. GC., "Exact solution for thermal boundary layer in casson fluid flow over permeable shrinking sheet with variable wall temperature and thermal radiation," (2016).
3. A. IL, A. EA, and F. Al., "Casson fluid flow with variable thermo-physical property along exponentially stretching sheet with suction and exponentially decaying internal heat generation using the homotopy analysis method," J. Nigerian Math Soc. **3** (2019).
4. Q. MZA, A. K, I. MF, and et al., "Heat and mass transfer analysis of unsteady non-newtonian fluid flow between porous surfaces in the presence of magnetic nanoparticles," Porous Media (2022).
5. A. K, W. Z, and H. Z., "Heat transfer analysis for casson fluid flow over stretching sheet with newtonian heating and viscous dissipation," 1127 (2019).
6. H. Waqas, M. Imran, and M. M. Bhatti, "Bioconvection aspects in non-newtonian three-dimensional carreau nanofluid flow with cattaneo-christov model and activation energy," The European Physical Journal Special Topics **5**, 1317–1330 (2021).
7. B. Mahanthesh and B. J. Gireesha, "Scrutinization of thermal radiation, viscous dissipation and joule heating effects on marangoni convective two-phase flow of casson fluid with fluid-particle suspension," Results **8**, 869–878 (2018).
8. M. R. Mohaghegh and A. B. Rahimi, "Tree-dimensional stagnation-point flow and heat transfer of a dusty fluid toward a stretching sheet," J. Heat Transfer **138(11)**, 112001 HT–15–1504 (2016).
9. T. Sajid, Z. Sabir, S. Tanveer, A. Arbi, and G. C. Altamirano, "Upshot of radiative rotating prandti fluid flow over a slippery surface embedded with variable species diffusivity and multiple convective boundary conditions," Heat Transfer **50(3)**, 2874–2 (2020).
10. T. Sajid, M. Sagheer, and S. Hussain, "Impact of temperature-dependent heat source/sink and variable species diffusivity on radiative reiner-philippof fluid," Math. Problems (2020).